Spectral Purification of Microwave Signals with Disciplined Dissipative Kerr Solitons

Wenle Weng,[1] Erwan Lucas,[1] Grigory Lihachev,[2,3] Valery E. Lobanov,[2] Hairun Guo,[1]
Michael L. Gorodetsky,[2,3] and Tobias J. Kippenberg[1,*]
[1]*École Polytechnique Fédérale de Lausanne (EPFL), CH-1015 Lausanne, Switzerland*
[2]*Russian Quantum Center, Skolkovo 143025, Russia*
[3]*Faculty of Physics, M.V. Lomonosov Moscow State University, 119991 Moscow, Russia*

(Received 2 August 2018; revised manuscript received 30 October 2018; published 3 January 2019)

Continuous-wave-driven Kerr nonlinear microresonators give rise to self-organization in terms of dissipative Kerr solitons, which constitute optical frequency combs that can be used to generate low-noise microwave signals. Here, by applying either amplitude or phase modulation to the driving laser we create an intracavity potential trap to discipline the repetition rate of the solitons. We demonstrate that this effect gives rise to a novel spectral purification mechanism of the external microwave signal frequency, leading to reduced phase noise of the output signal. We experimentally observe that the microwave signal generated from disciplined solitons is injection locked by the external drive at long timescales, but exhibits an unexpected suppression of the fast timing jitter. Counterintuitively, this filtering takes place for frequencies that are substantially lower than the cavity decay rate. As a result, while the long timescale stability of the Kerr frequency comb's repetition rate is improved by more than 4 orders of magnitude, the purified microwave signal shows a reduction of the phase noise by 30 dB at offset frequencies above 10 kHz.

DOI: 10.1103/PhysRevLett.122.013902

Introduction.—Low-noise microwave signals play a vital role in a wide range of industrial and scientific applications, including telecommunication networks [1], radar and LIDAR systems [2], as well as in fundamental research such as long baseline interferometry [3] and tests of fundamental constants [4,5]. Traditionally, the microwave signals with the best spectral purity were provided by cryogenic microwave oscillators [6,7]. Owing to the advancement of mode-locked-laser frequency combs and optoelectronics, new photonic-based ways of generating ultralow-noise microwaves have been proposed and demonstrated, such as optical frequency division [8–10], electro-optical frequency division [11], or Brillouin lasing in microresonators [12,13].

Recently, dissipative Kerr solitons (DKS) in optical microresonators [14,15] have been attracting surging interests thanks to their self-organizing mechanism that results from the double-balance between nonlinearity and anomalous dispersion, as well as between parametric gain and cavity loss. DKS offer high coherence, broad bandwidth and microwave-repetition rate frequency combs (also referred to as soliton microcombs [16]), and have been applied successfully to ultrafast ranging [17,18], dual-comb spectroscopy [19–21], calibrating astrophysical spectrometer [22,23], as well as optical frequency synthesis [24]. Like mode-locked-laser frequency combs, soliton microcombs can function as a frequency link between the microwave or radio-frequency (rf) domain and the optical domain [25,26]. In particular, microcomb-based microwave oscillators hold great promise of providing a robust, portable, and power-efficient way to synthesize pure microwave tones [27]. In contrast to microresonator-based approaches of generating microwave signals using Brillouin lasers, the frequency of the generated signal is mainly determined by the cavity free spectral range (FSR), rather than the host material property of the resonator, thus offering control over the microwave center frequency. However, this flexibility comes at a price: reaching a good long-term stability requires the ability to control the comb repetition rate (f_{rep}) and the carrier-envelope offset (f_{ceo}) and discipline them to optical references or rf clocks. To obtain such ability most previous efforts focused on using active feedback to correct thermal drifts and noises [28,29] and utilizing sophisticated structure design for appropriate actuation [26,30,31].

In this work, we use DKS in a crystalline microresonator to purify a 14.09 GHz microwave signal. The phase noise of the purified signal approaches −130 dBc/Hz at 10 kHz offset frequency, which is at the level achieved by the state-of-the-art microresonator-based optoelectronic oscillators and the previously reported best results obtained with undisciplined DKS and narrow-band rf filter [2,27]. We adapt the microwave injection-locking technique that was previously used to stabilize modulation-instability (MI) combs [25,32] to discipline the soliton stream by creating intracavity potential gradient that traps the solitons. This mechanism not only relies on linear cavity filtering, but exploits further the dynamics of DKS, and allows us to reduce substantially the phase noise of an external microwave drive. Owing to the dynamical attractor of the soliton state, the stability of the disciplined solitons exhibits strong robustness against incoherent perturbations contained in

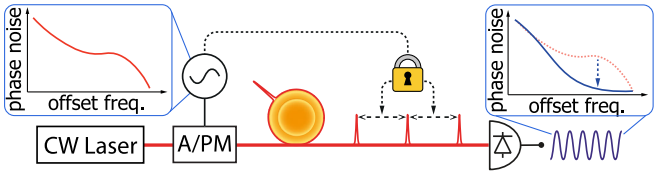

FIG. 1. The concept of a microcomb-based microwave spectral purifier. A commercially available electronic microwave oscillator (Rohde&Schwarz SMB100A) is used to modulate the pump laser, leading to the injection locking of solitons, thus providing a long-term frequency reference to the soliton repetition rate. The generated microwave exhibits a reduced phase noise level due to the nonlinear soliton dynamics, leading to noise reduction of the microwave signal for Fourier frequencies far away from the carrier.

the injected signals [33], thus efficiently dissipating noises in a coherent system. This self-purifying mechanism leads to the reduction of the injected microwave phase noise, allowing the nonlinear cavity in the soliton state to act as a passive spectral purifier that can improve the performance of an external off-the-shelf electronic oscillator. As depicted in Fig. 1, the disciplined-DKS-based microwave purifier constitutes in itself a f_{rep}-stabilized frequency comb and a spectrally pure microwave generator into a single device.

Experiment.—The experimental setup is shown in Fig. 2(a). A 1555-nm laser is amplified by an Erbium-doped fiber amplifier (EDFA) and 200 mW optical power is coupled into a z-cut magnesium fluoride (MgF_2) whispering-gallery-mode resonator with a FSR of 14.09 GHz via a tapered fiber. A single-soliton-state DKS comb is generated by scanning the laser over a resonance with a loaded quality factor (Q) of 1.3×10^9 to reach the steplike range where solitons are formed [14]. To stabilize the effective laser detuning with respect to the cavity resonance, we apply phase modulation to the laser with an electro-optic modulator (EOM) to generate Pound-Drever-Hall (PDH) error signals. The laser frequency is locked to the high-frequency PDH sideband by setting the lock point of the servo to the center of the sideband resonance which is indicated in Fig. 2(e). The frequency of the laser is then compared with a tooth of a stabilized fiber-laser-based comb, and the frequency difference is stabilized at 20 MHz through a slow thermal actuation on the cavity by active control of the pump power with an acousto-optic modulator (AOM). As illustrated in Fig. 2(c), with the two servos this "prestabilization" scheme stabilizes both the pump laser frequency and the pump-cavity detuning. As a result, the stability of f_{rep} is improved by up to 2 orders of magnitude at timescales of >10 s [see Fig. 2(f)], allowing the time-consuming measurement of phase noise via cross-correlation to be carried out properly. One should note that the fiber-laser-based comb can be replaced with a laser stabilized by a reference cavity [34] or an atomic vapor cell [35], and that with improved thermal isolation [27] or self-referenced stabilization [36] the entire setup can be more compact.

The injection locking of the soliton repetition rate is implemented by applying amplitude modulation (AM) or phase modulation (PM) on the pump laser, at a frequency close to the FSR. Intuitive illustrations of how the injection locking works are presented in Figs. 3(a) and 3(b). From a frequency domain perspective, the modulation frequency defines f_{rep} through parametric four-wave-mixing. In the time domain, a modulated cw field traps solitons and disciplines f_{rep} correspondingly. In this proof-of-principle experiment we use a synthesizer to drive the AM/PM modulator but the input microwave signal could be derived from a frequency-multiplied clock oscillator or a voltage-controlled oscillator (VCO). The modulation frequency f_{mod} is swept around the free-running f_{rep} (~14.09 GHz) and we observe that f_{rep} is injection locked by the input microwave signal. Figure 3(c) shows the evolution of the microwave spectrum of the DKS as we slowly swept the AM f_{mod}. When the difference between f_{mod} and

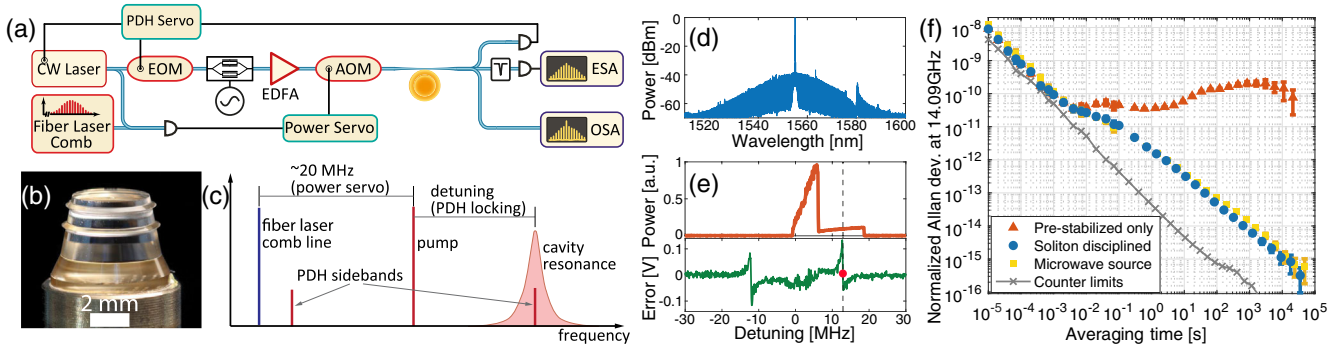

FIG. 2. (a) The experimental setup. (b) The MgF_2 resonator used in the experiment. (c) Illustration of the PDH offset locking and the prestabilization scheme. (d) Optical spectrum of the soliton microcomb. (e) Generated comb power as the laser is scanned across the pumped resonance (upper) and the corresponding PDH error signal (lower). The red dot indicates the locking point. (f) Allan deviations of f_{rep} when the Kerr comb is prestabilized and DKS-disciplined, respectively. We counted f_{rep} with a Π-type frequency counter that is referenced to the same frequency source (relative frequency instability $< 1 \times 10^{-12}$ at 1 s averaging time) to which f_{mod} is referenced.

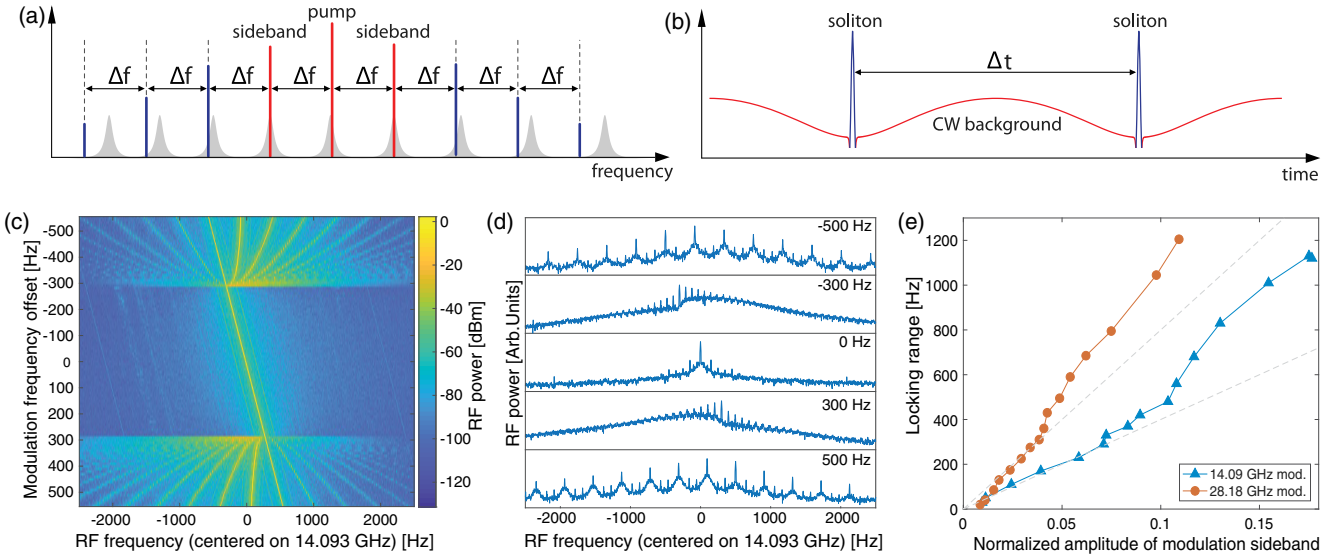

FIG. 3. (a) In frequency domain, the difference between the pump laser and the modulated sidebands sets the microcomb f_{rep}. (b) In time domain, the potential of the modulated cw field traps solitons, thus locking f_{rep} of the soliton train. (c) Evolution of the spectrum around 14.09 GHz. (d) Snapshots with different f_{mod} detuned from free-running f_{rep} (indicated in the upper-right corners) showing the typical states of unlocked (−500 and 500 Hz), quasilocked (−300 and 300 Hz), and injection-locked (0 Hz). (e) Locking ranges with varied AM strengths for modulation frequencies around f_{rep} (blue circles) and $2 \times f_{rep}$ (red circles), respectively.

the free-running f_{rep} is larger than ∼400 Hz, multiple spectral components including f_{mod} (the strongest), f_{rep} (the second strongest) and multiple harmonics are observed in the spectra, indicating an absence of injection locking. As f_{mod} is approaching the free-running f_{rep}, the spectrum displays a typical frequency-pulling effect as f_{rep} is pulled towards f_{mod} [37]. When the difference between f_{mod} and free-running f_{rep} is less than ∼300 Hz all the spectral components merge into a major one, indicating that the f_{rep} is synchronized to f_{mod}; i.e., the soliton stream is locked to the external drive. We measured the frequency instabilities of the injected-locked f_{rep} against f_{mod}, which is also presented in Fig. 2(f). The Allan deviation shows that at time scales of >0.1 s the fluctuations of f_{rep} has been suppressed significantly—up to more than 4 orders of magnitude at averaging time of 1000 s, indicating that the disciplined DKS tightly follow the injected microwave frequency.

We acquire the locking range from the evolution of the rf spectrum, and repeat the measurement with varied modulation strength. As shown in Fig. 3(e), with the normalized amplitude of the modulation sideband below 0.07, the locking range rises monotonically with almost perfect linearity as the modulation strength increases. With stronger modulation the slope of the locking range scaling increases, which is attributed to the appearance of higher-order modulation sidebands that increase the gradient of the potential and trap the solitons more effectively [38–41]. For the same reason, we observe that the locking range increases by nearly a factor of 2 when we measure the locking range with f_{mod} around $2 \times f_{rep}$ (∼28.18 GHz).

Spectral purification effect.—To characterize the spectral purity at f_{rep}, the out-coupled soliton stream is filtered by fiber Bragg grating filters (FBG) to suppress the pump light and then amplified by an EDFA and subsequently attenuated to ∼5 mW before being registered by a fast photodetector. We use a phase noise analyzer to measure the phase noise of the 14.09 GHz signal output by the photodetector. Figure 4 presents the single-sideband (SSB) phase noise level when PM injection locking was performed. One should note that very similar results were

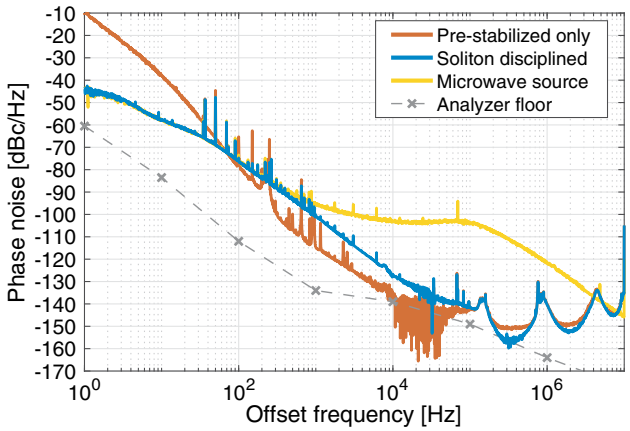

FIG. 4. Phase noise spectra of the soliton repetition rate with and without PM injection locking. The phase noise of the input microwave signal is also presented, showing that the injection locking reduces the noise level by nearly 40 dB for offsets at 100 kHz. The crosses and the dashed line show the noise floor of the phase noise analyzer.

also observed with AM injection locking. At low offset frequencies between 1 and 100 Hz the injection-locked DKS show an improved noise level that is in agreement with the phase noise level of the input rf tone due to the better long-term frequency stability provided by the injected microwave signal, as confirmed by the Allan deviations. This result shows that the soliton stream is strictly disciplined by the potential trap at low frequency ranges. Remarkably, at offset above 100 Hz the spectrum of the injection-locked f_{rep} mostly maintains the intrinsic high quality, which is several orders of magnitude lower than the input microwave in terms of phase noise level. We note that this purifying effect cannot be explained by the cavity filtering since the frequency range where the purification is observed is ~3 orders of magnitude lower than the loaded cavity resonance bandwidth (~150 kHz). At offset frequencies above 30 kHz a reduction of the input microwave phase noise level by 30 dB is achieved, showing the exceptional spectral purifying ability of the disciplined DKS.

Simulation of soliton spectral purification.—In order to study the mechanism of the observed spectral purification, we performed simulations of PM-to-PM transfer function based on the Lugiato-Lefever equation (LLE) [42]. The model is similar to the one described in Ref. [43], which is expressed as

$$\frac{\partial \tilde{A}_\mu(t)}{\partial t} = \left(-\frac{\kappa}{2} + i(2\pi\delta) + iD_{\mathrm{int}}(\mu)\right)\tilde{A}_\mu - ig\mathcal{F}[|A|^2A]_\mu + \sqrt{\kappa_{\mathrm{ex}}}s_{\mathrm{in}}\left(\delta'_{\mu 0} + \delta'_{\mu\pm1}i\frac{\epsilon}{2}e^{\pm i\Omega t}\right), \tag{1}$$

where $\tilde{A}_\mu$ and A are the spectral and temporal envelopes of DKS, respectively, (related via $A(t) = \sum_\mu \tilde{A}_\mu e^{-i\mu D_1 t}$), κ is the cavity loss rate, g is the single photon induced Kerr frequency shift, κ_{ex} is the coupling rate and $|s_{\mathrm{in}}|^2$ denotes the power of the laser pumping the central mode, $\delta'_{\mu 0/\pm 1}$ is the Kronecker delta, and $\mathcal{F}[]_\mu$ represents the μth frequency component of the Fourier series. We include third order dispersion in $D_{\mathrm{int}}(\mu)$. A pair of PM sidebands are included in the last term of the equation, where ϵ indicates the amplitude of the modulation sidebands, and Ω is the frequency difference between the FSR and the input microwave signal.

Adapting the technique used in Ref. [44], we introduce phase modulation on the microwave signal with phase deviation of 0.1 radian and varied modulation frequencies from 200 Hz to 1 MHz. The phases of the purified microwave signal can be derived from the comb spectra with

$$\Psi(t) = \mathrm{Arg}\left(e^{i\omega_{\mathrm{in}}t}\sum_\mu \tilde{A}_\mu \tilde{A}^\dagger_{\mu-1}\right), \tag{2}$$

where ω_{in} is the frequency of the input microwave signal. We use pump power of 200 mW and $\epsilon = 0.32$ for the numerical simulation [45]. The results are presented in Fig. 5. The simulated transfer function follows a typical first-order low-pass filtering effect, showing a magnitude that is close to unity at low frequency (200 Hz). For higher offset frequencies the magnitude decreases with a slope of −20 dB/decade, reaching a minimum of ~−63 dB around 500 kHz, thus revealing a significant phase noise suppression in the soliton state. To verify the simulated results, we apply PM with varied phase deviation on the injected microwave signal and record the resulting phase deviation on the soliton repetition rate with an in-phase-and-quadrature (IQ) demodulator [45]. The experimentally measured transfer functions are plotted in the same figure. From the comparison we see that at low frequencies the experimental results and the simulation are in satisfactory agreement. However, at frequencies above ~100 kHz the experimental curves show flat floors, which are attributed to the detection noise floor introduced by the analyzer we use to perform the measurement. This instrumental noise floor is confirmed by increasing the modulation strength, which improves the dynamic range of our measurement.

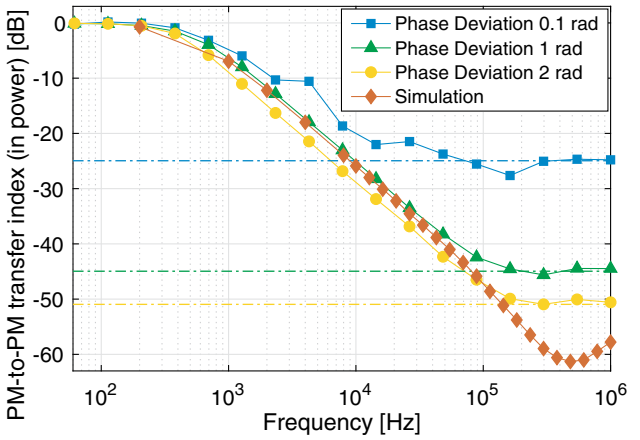

FIG. 5. Experimentally measured and numerically simulated phase noise transfer indices for the PM-to-PM noise transfer from injected microwave signal to f_{rep} of the DKS stream. The flat floors of the experimental data at frequencies above 100 kHz are due to the noise floor of the phase noise analyzer during the IQ measurement, which are indicated by the dash-dot lines.

Conclusion.—We have experimentally and numerically demonstrated a novel phase noise purifying mechanism by disciplining dissipative solitons with potential traps. The comb repetition rate drift, which is a major limitation in microcavities, was thereby suppressed, while this parameter was stabilized to a reference oscillator. The high frequency noise of the trapping signal was self-purified, at frequency offsets well below the cavity resonance bandwidth. Our technique reveals the unique dynamical stability of the self-organized temporal solitons. The exceptional phase noise level achieved with the purified microwaves shows that disciplined DKS are competitive with other state-of-the-art optical-microresonator-based microwave oscillators in terms of generating low-noise microwave signals with a

miniaturized device. It could also facilitate the application of microcombs in coherently averaged dual-comb spectroscopy [49] and coherent optical telecommunication [50].

The code and data used to produce the plots within this Letter are available by following the link in Ref. [51].

This publication was supported by Contract No. D18AC00032 (DRINQS) from the Defense Advanced Research Projects Agency (DARPA), Defense Sciences Office (DSO), and funding from the Swiss National Science Foundation under Grant Agreements No. 163864 and No. 165933, and by the Russian Foundation for Basic Research under Project No. 17-02-00522. W. W. acknowledges support by funding from the European Union's Horizon 2020 research and innovation programme under Marie Sklodowska-Curie IF Grant Agreement No. 753749 (SOLISYNTH).

W. W. and E. L. contributed equally to this work.

*tobias.kippenberg@epfl.ch

[1] D. M. Pozar, *Microwave and RF Design of Wireless Systems* (Wiley, New York, 2001).
[2] L. Maleki, Nat. Photonics **5**, 728 (2011).
[3] S. Grop, P. Bourgeois, N. Bazin, Y. Kersalé, E. Rubiola, C. Langham, M. Oxborrow, D. Clapton, S. Walker, J. De Vicente *et al.*, Rev. Sci. Instrum. **81**, 025102 (2010).
[4] P. L. Stanwix, M. E. Tobar, P. Wolf, M. Susli, C. R. Locke, E. N. Ivanov, J. Winterflood, and F. van Kann, Phys. Rev. Lett. **95**, 040404 (2005).
[5] M. Nagel, S. R. Parker, E. V. Kovalchuk, P. L. Stanwix, J. G. Hartnett, E. N. Ivanov, A. Peters, and M. E. Tobar, Nat. Commun. **6**, 8174 (2015).
[6] S. Grop, P.-Y. Bourgeois, R. Boudot, Y. Kersalé, E. Rubiola, and V. Giordano, Electron. Lett. **46**, 420 (2010).
[7] J. G. Hartnett, N. R. Nand, and C. Lu, Appl. Phys. Lett. **100**, 183501 (2012).
[8] T. M. Fortier, M. S. Kirchner, F. Quinlan, J. Taylor, J. Bergquist, T. Rosenband, N. Lemke, A. Ludlow, Y. Jiang, C. Oates *et al.*, Nat. Photonics **5**, 425 (2011).
[9] F. Quinlan, T. M. Fortier, H. Jiang, A. Hati, C. Nelson, Y. Fu, J. C. Campbell, and S. A. Diddams, Nat. Photonics **7**, 290 (2013).
[10] X. Xie, R. Bouchand, D. Nicolodi, M. Giunta, W. Hänsel, M. Lezius, A. Joshi, S. Datta, C. Alexandre, M. Lours *et al.*, Nat. Photonics **11**, 44 (2017).
[11] J. Li, X. Yi, H. Lee, S. A. Diddams, and K. J. Vahala, Science **345**, 309 (2014).
[12] J. Li, H. Lee, and K. J. Vahala, Nat. Commun. **4**, 2097 (2013).
[13] W. Loh, J. Becker, D. C. Cole, A. Coillet, F. N. Baynes, S. B. Papp, and S. A. Diddams, New J. Phys. **18**, 045001 (2016).
[14] T. Herr, V. Brasch, J. Jost, C. Wang, N. Kondratiev, M. Gorodetsky, and T. Kippenberg, Nat. Photonics **8**, 145 (2014).
[15] N. Akhmediev and A. Ankiewicz, in *Dissipative Solitons* (Springer, Berlin, 2005), pp. 1–17.
[16] T. J. Kippenberg, A. L. Gaeta, M. Lipson, and M. L. Gorodetsky, Science **361**, eaan8083 (2018).
[17] P. Trocha, M. Karpov, D. Ganin, M. H. Pfeiffer, A. Kordts, S. Wolf, J. Krockenberger, P. Marin-Palomo, C. Weimann, S. Randel *et al.*, Science **359**, 887 (2018).
[18] M.-G. Suh and K. J. Vahala, Science **359**, 884 (2018).
[19] M.-G. Suh, Q.-F. Yang, K. Y. Yang, X. Yi, and K. J. Vahala, Science **354**, 600 (2016).
[20] N. Pavlov, G. Lihachev, S. Koptyaev, E. Lucas, M. Karpov, N. Kondratiev, I. Bilenko, T. Kippenberg, and M. Gorodetsky, Opt. Lett. **42**, 514 (2017).
[21] A. Dutt, C. Joshi, X. Ji, J. Cardenas, Y. Okawachi, K. Luke, A. L. Gaeta, and M. Lipson, Sci. Adv. **4**, e1701858 (2018).
[22] M.-G. Suh, X. Yi, Y.-H. Lai, S. Leifer, I. S. Grudinin, G. Vasisht, E. C. Martin, M. P. Fitzgerald, G. Doppmann, J. Wang *et al.*, Nat. Photonics **13**, 25 (2019).
[23] E. Obrzud, M. Rainer, A. Harutyunyan, M. Anderson, M. Geiselmann, B. Chazelas, S. Kundermann, S. Lecomte, M. Cecconi, A. Ghedina *et al.*, Nat. Photonics, **13**, 31 (2018).
[24] D. T. Spencer, T. Drake, T. C. Briles, J. Stone, L. C. Sinclair, C. Fredrick, Q. Li, D. Westly, B. R. Ilic, A. Bluestone *et al.*, Nature (London) **557**, 81 (2018).
[25] S. B. Papp, K. Beha, P. Del'Haye, F. Quinlan, H. Lee, K. J. Vahala, and S. A. Diddams, Optica **1**, 10 (2014).
[26] P. Del'Haye, A. Coillet, T. Fortier, K. Beha, D. C. Cole, K. Y. Yang, H. Lee, K. J. Vahala, S. B. Papp, and S. A. Diddams, Nat. Photonics **10**, 516 (2016).
[27] W. Liang, D. Eliyahu, V. S. Ilchenko, A. A. Savchenkov, A. B. Matsko, D. Seidel, and L. Maleki, Nat. Commun. **6**, 7957 (2015).
[28] J. Jost, E. Lucas, T. Herr, C. Lecaplain, V. Brasch, M. Pfeiffer, and T. Kippenberg, Opt. Lett. **40**, 4723 (2015).
[29] S.-W. Huang, J. Yang, M. Yu, B. H. McGuyer, D.-L. Kwong, T. Zelevinsky, and C. W. Wong, Sci. Adv. **2**, e1501489 (2016).
[30] S. B. Papp, P. Del'Haye, and S. A. Diddams, Phys. Rev. X **3**, 031003 (2013).
[31] J. Lim, A. A. Savchenkov, E. Dale, W. Liang, D. Eliyahu, V. Ilchenko, A. B. Matsko, L. Maleki, and C. W. Wong, Nat. Commun. **8**, 8 (2017).
[32] S. B. Papp, P. Del'Haye, and S. A. Diddams, Opt. Express **21**, 17615 (2013).
[33] F. Leo, S. Coen, P. Kockaert, S.-P. Gorza, P. Emplit, and M. Haelterman, Nat. Photonics **4**, 471 (2010).
[34] D. G. Matei, T. Legero, S. Häfner, C. Grebing, R. Weyrich, W. Zhang, L. Sonderhouse, J. M. Robinson, J. Ye, F. Riehle, and U. Sterr, Phys. Rev. Lett. **118**, 263202 (2017).
[35] W. Liang, A. A. Savchenkov, V. S. Ilchenko, D. Eliyahu, A. B. Matsko, and L. Maleki, IEEE Photonics J. **9**, 5502411 (2017).
[36] W. Weng, J. D. Anstie, P. Abbott, B. Fan, T. M. Stace, and A. N. Luiten, Phys. Rev. A **91**, 063801 (2015).
[37] B. Razavi, IEEE J. Solid-State Circuits **39**, 1415 (2004).
[38] H. Taheri, A. B. Matsko, and L. Maleki, Eur. Phys. J. D **71**, 153 (2017).
[39] H. Taheri, A. A. Eftekhar, K. Wiesenfeld, A. Adibi, IEEE Photonics J. **7**, 2200309 (2015).
[40] J. K. Jang, M. Erkintalo, S. Coen, and S. G. Murdoch, Nat. Commun. **6**, 7370 (2015).
[41] V. E. Lobanov, G. Lihachev, and M. L. Gorodetsky, Europhys. Lett. **112**, 54008 (2015).

[42] L. A. Lugiato and R. Lefever, Phys. Rev. Lett. **58**, 2209 (1987).
[43] H. Guo, E. Lucas, M. H. P. Pfeiffer, M. Karpov, M. Anderson, J. Liu, M. Geiselmann, J. D. Jost, and T. J. Kippenberg, Phys. Rev. X **7**, 041055 (2017).
[44] A. B. Matsko and L. Maleki, J. Opt. Soc. Am. B **32**, 232 (2015).
[45] See Supplemental Material at http://link.aps.org/supplemental/10.1103/PhysRevLett.122.013902 for details, which also includes Refs. [43,44,46–48].
[46] X. Yi, Q.-F. Yang, X. Zhang, K. Y. Yang, X. Li, and K. Vahala, Nat. Commun. **8**, 14869 (2017).
[47] Y. Wang, F. Leo, J. Fatome, M. Erkintalo, S. G. Murdoch, and S. Coen, Optica **4**, 855 (2017).
[48] E. Lucas, H. Guo, J. D. Jost, M. Karpov, and T. J. Kippenberg, Phys. Rev. A **95**, 043822 (2017).
[49] I. Coddington, N. Newbury, and W. Swann, Optica **3**, 414 (2016).
[50] P. Marin-Palomo, J. N. Kemal, M. Karpov, A. Kordts, J. Pfeifle, M. H. Pfeiffer, P. Trocha, S. Wolf, V. Brasch, M. H. Anderson *et al.*, Nature (London) **546**, 274 (2017).
[51] See https://doi.org/10.5281/zenodo.2222431.